PAPER

Analysis of anisotropic effects on energy induced by lower hybrid wave heating on EAST

IOP Publishing Plasma Physics and Controlled Fusion
Plasma Phys. Control. Fusion 59 (2017) 065010 (6pp) https://doi.org/10.1088/1361-6587/aa6988

Analysis of anisotropic effects on energy induced by lower hybrid wave heating on EAST

J Huang[1,2,4], Y Liang[1,3], J P Qian[1], L Q Xu[1], K Y He[1,2], Y K Liu[1,2] and the EAST team

[1] Institute of Plasma Physics, Chinese Academy of Sciences, Hefei 230031, People's Republic of China
[2] University of Science and Technology of China, Hefei, 230026, People's Republic of China
[3] Forschungszentrum Juelich GmbH, Association EURATOM-FZ Juelich, Institut fuer Energieforschung—Plasmaphysik, Trilateral Euregio Cluster, D-52425 Juelich, Germany

E-mail: jiehuang@ipp.ac.cn

Received 6 November 2016, revised 22 March 2017
Accepted for publication 28 March 2017
Published 4 May 2017

Abstract

It has been pointed out that plasma anisotropy has a significant impact on the characteristics of magnetohydrodynamic equilibrium and instability. Recently, anisotropic pressure effects induced by 4.6 GHz lower hybrid wave (LHW) heating on the Experimental Advanced Superconducting Tokamak (EAST) has been investigated. The mechanism is due to the high-energy electrons generated by LHW Landau damping effects in the direction parallel to the magnetic field line.

Keywords: anisotropy, LHW heating, EAST

(Some figures may appear in colour only in the online journal)

1. Introduction

Auxiliary heating is required for D-T ignition in future tokamak fusion power plants, as ohmic heating is less effective at high temperature. Nevertheless, unlike ohmic global heating, the auxiliary heating could raise new questions as it can give rise to ion or electron velocity distributions that are non-Maxwell, which may be the key factor of the decreasing energy confinement time scale with increasing power [1]. In tokamaks, due to the particle travel along the magnetic field line, the parallel scale lengths can be much longer than the perpendicular one [2], easily leading to different properties in the plasma parameters in different directions. When the losing time scales of high-energy particle produced by auxiliary heating is longer than the confinement time scales, it will induce the anisotropic plasma, which is $P_{\perp} \neq P_{||}$. Here $P_{\perp}$ and $P_{||}$ denote the plasma pressure perpendicular and parallel to the magnetic field, respectively.

Recently there has been lots of work related to the study pressure anisotropy [3–5] and its effects on stability, such as internal kink mode [6], resistive wall mode [7], and Alfvén eigenmode [8]. It has been pointed out that the characteristics of magnetohydrodynamic (MHD) equilibrium and instability under anisotropic pressure are different from those under isotropic pressure. Therefore, a quantitative evaluation of the plasma anisotropy is important for the study of MHD equilibrium and instability.

As auxiliary heating can give rise to velocity distributions that are non-Maxwell, it has been reported that anisotropy usually appears in the magnetic confinement fusion plasma with ion cyclotron resonance heating (ICRH) or neutral beam injection (NBI) heating, especially in high β and low n_e discharges. The anisotropy magnitude can reach $p_{\perp}/p_{||} \sim 2.5$ with ICRH [9] on JET. And on MAST, it can reach $p_{\perp}/p_{||} \sim 1.7$ during NBI heating [10]. Recently, the pressure anisotropic effects on energy induced by the 4.6 GHz LHW heating on EAST was observed for the first time.

In theory, LHW are potential sources to heat both electrons and ions to the thermonuclear temperature under Landau damping [11]. In particular, LHW can generate the noninductive current in tokamaks, which may contribute to the steady-state operation [12]. In present day experiments, LHW are often used for electron heating and play an important role in current drive and profile control [13]. Through wave-particle resonance in the

[4] Author to whom any correspondence should be addressed.

direction parallel to the magnetic field line, LHW can lead to strong quasilinear Landau interaction with electrons, and consequently to electron heating and non-inductive current drive [14]. In addition, LHW will induce the anisotropic plasma as it can give rise to high-energy electrons in the parallel direction. In other words, the double of plasma parallel energy is not the same with perpendicular energy. As an expected result, the anisotropic degree may have dependence on the electron density, the LHW heating power and the background electron temperature since the density is related to the collision frequency. Also, the density and the background electron temperature will have an impact on LHW heating efficiency.

In this paper, instead of calculating the pressure profile in a different direction, we focus on the pressure anisotropic effects on energy distribution induced by the 4.6 GHz LHW heating on EAST. Section 2 outlines the energy calculation method. Section 3 presents the calculation results of the anisotropic effects on energy, and its dependence on the heating power or the line averaged electron density. The influence of electron temperature on the anisotropic pressure is also discussed in section 3. Conclusions of the experimental results will be summarized in section 4.

2. Experimental method

EAST, as a full superconducting tokamak, is aimed at long-pulse stable high-performance H-modes plasma with ITER-like configuration and heating schemes. EAST has a flexible selection of lower single null (LSN), upper single null (USN) or double null (DN) poloidal divertor configurations and circular configurations with a limiter. Major radius and minor radius of EAST are $R = 1.85$ m and $a = 0.45$ m, respectively [15]. For steady-state plasma with LHCD, a new 4.6 GHz LHW system with an array of 24 (four rows and six columns) waveguide antennas has been firstly commissioned on EAST in the 2014 experimental campaign [16].

To study the anisotropic degree induced by LHW heating, two kinds of energy (W_{mhd} and W_{dia}) have been calculated. Here W_{mhd} is the plasma energy calculated by the EFIT code [17], and W_{dia} is one and a half times the total plasma perpendicular thermal energy measured by the diamagnetic loop on EAST. Assuming both the magnetic and diamagnetic measurements are accurate, then the difference of W_{mhd} and W_{dia} provides an estimate of pressure anisotropic degree.

Based on Picard iteration, EFIT calculation uses the least-squares method to directly solve the Grad–Shafranov equation numerically with the kinetic profiles represented by truncated polynomial functions. The EFIT method can effectively rebuild tokamak plasma equilibrium configuration, the plasma current profile and other balance parameters [18]. In the EFIT calculation, the volume-dependent parameters can be accurately obtained from measured external poloidal magnetic field and flux values by approximating the plasma current distribution. Hence the accuracy of the W_{mhd} depends on how accurately the constrains form magnetic measurement, and it is reliable even in the anisotropic pressure plasma for a shaped tokamak [19].

The diamagnetic loop measures the toroidal diamagnetic flux which is related to the poloidal beta and the total perpendicular thermal energy of the plasma ($W_{\perp}$). The relation between the poloidal beta and the diamagnetic flux is derived from simplified equilibrium relation:

$$\beta_{\mathrm{p}} = 1 - \frac{8\pi B_{\mathrm{T}}}{(\mu_0 I_{\mathrm{p}})^2}\Delta\phi_{\mathrm{dia}}. \tag{1}$$

The volume averaged plasma kinetic pressure $\langle p\rangle$ can be measured directly from the definition of the poloidal beta:

$$\langle p\rangle = \beta_{\mathrm{p}}\frac{B_{\theta}^2(a)}{2\mu_0}. \tag{2}$$

Then the stored energy W_{dia} can be obtained:

$$W_{\mathrm{dia}} = \frac{3}{2}\left(\sum\nolimits_{\alpha} n_{\alpha}T_{\alpha}\right)V = \frac{3}{2}\langle P\rangle V \tag{3}$$

where V is the plasma volume.

With W_{mhd} and W_{dia}, the plasma parallel energy ($W_{||}$) and the plasma perpendicular thermal energy ($W_{\perp}$) can be expressed as:

$$W_{\perp} = \frac{2}{3}W_{\mathrm{dia}} \tag{4}$$

$$W_{\parallel} = W_{\mathrm{mhd}} - \frac{2}{3}W_{\mathrm{dia}} \tag{5}$$

By comparing the discrepancy between W_{mhd} and W_{dia} (or $2^{*}W_{\parallel}$ versus $W_{\perp}$), the degree of the anisotropic effects on energy and its dependence on the power or the density can be obtained with statistical methods. Note, $W_{||} = 0.5W_{\perp}$ in the case of isotropic pressure. Here we define the anisotropic effects factor:

$$\sigma = 2^{*}W_{\parallel}/W_{\perp}. \tag{6}$$

In this paper, the anisotropic effects on energy induced by the 4.6 GHz LHW system are presented, in which the toroidal magnetic field (B_{t}) is about 2.3 T and the configuration is LSN. The experimental primary working gas is deuterium (D_2) and all these calculation shots are L mode. W_{mhd} and W_{dia} are the average value of 0.5 s, which are calculated from the discharge plateau region for each shot.

3. Statistical properties of the anisotropic effects on energy

3.1. The density dependence of the anisotropic effects on energy

In figure 1 the electron density dependence of W_{mhd} and W_{dia} and their discrepancy are presented. In the figure we selected 61 shots from the recent experimental campaign database in such a way that all these shots are L mode and have the same I_{P}, B_{t}, heating power and LSN poloidal divertor configuration. As the density increases from $1.1 \times 10^{19}\,\mathrm{m}^{-3}$ to $3.3 \times 10^{19}\,\mathrm{m}^{-3}$, W_{dia} increases while W_{mhd} decreases. In addition, the increase rate of W_{dia} is larger than the W_{mhd} decline rate. According to the measurement method, the W_{dia} increase represents the plasma perpendicular energy ($W_{\perp}$) increase with density increase. As a result, the increasing perpendicular energy ($W_{\perp}$) and decreasing total energy (W_{mhd}) means the plasma parallel energy ($W_{||}$)

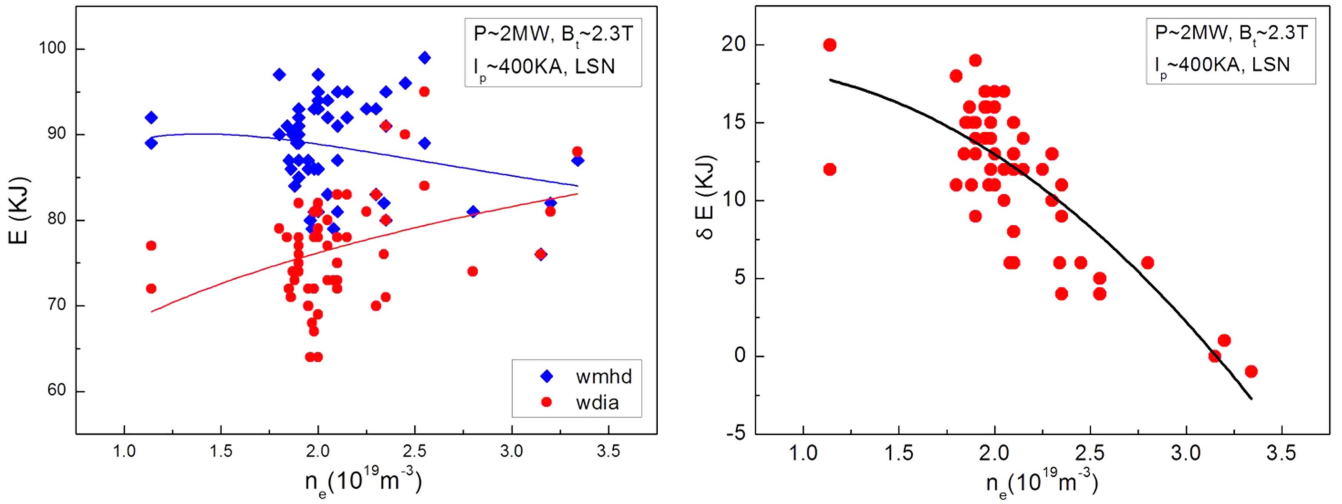

Figure 1. Density dependence of W_{mhd}, W_{dia} and δE. Here $\delta E = W_{mhd} - W_{dia}$. In these shots, the toroidal magnetic field is about 2.3 T, the plasma current is about 400 KA, the 4.6 GHz heating power is about 2 MW and the configuration is LSN.

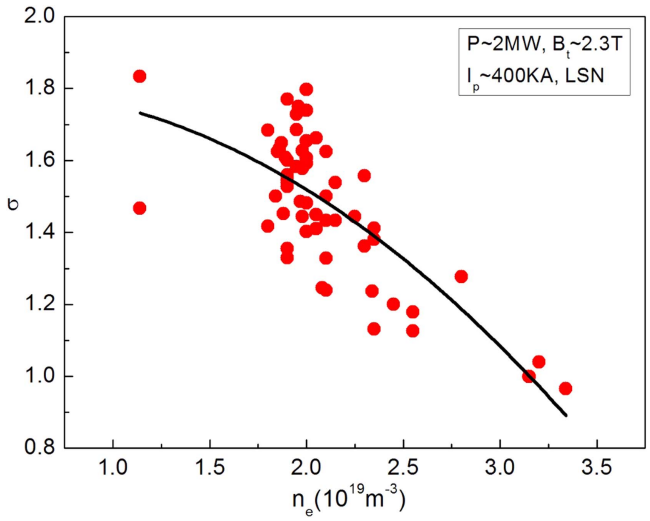

Figure 2. Density dependence of the anisotropic effects on energy. Here the anisotropic factor σ is the ratio of double parallel and perpendicular components of the plasma energy. In these shots, the toroidal magnetic field is about 2.3 T, the plasma current is about 400 KA, the 4.6 GHz heating power is about 2 MW and the configuration is LSN.

decreases with the density increase. The discrepancy between W_{mhd} and W_{dia} can reach $\delta E \sim 20$ KJ at low density.

The statistical properties of the density dependence of the anisotropic effects on energy are shown in figure 2. It is obvious that an increase in anisotropic degree is correlated with a decrease in density. And the anisotropic factor can reach $\sigma \sim 1.8$ at low density.

3.2. Heating power dependence of the anisotropic effects on energy

W_{mhd} and W_{dia} and their discrepancy dependence on LHW heating power is shown in figure 3. In this case, we selected 93 shots from the recent experimental campaign. All these shots are L mode and have the same I_P, B_t, n_e, and LSN poloidal divertor configuration. With the power increasing, both W_{mhd} and W_{dia} increase and the W_{mhd} increase rate is larger than the W_{dia} increase rate. As a result, the discrepancy between W_{mhd} and W_{dia} (δE) increases with power increase. Assuming that the plasma is isotropic in the ohmic discharge, W_{mhd} and W_{dia} should be equal. For ohmic discharges in the calculation (the data point of the LHW heating power is zero in the figure), the average calculation of W_{mhd} is about 2 KJ less than W_{dia}, and the fluctuation amplitude of δE is about 10 KJ. The 2 KJ deviation may be due to the calibration of the diamagnetic flux measurement. In the W_{dia} measurement, since the diamagnetic loop may not be strictly installed in the poloidal plan, the poloidal flux may also have an impact on the toroidal flux measurement value. Hence the diamagnetic flux should be corrected as $\Delta\phi_{dia} = \Delta\phi_{Dia} - \alpha I_{PF} - \beta I_{RMP} - \gamma I_p$ to eliminate the poloidal flux influence (here, $\Delta\phi_{Dia}$ represents the measurement value, $\Delta\phi_{dia}$ represents the true value. And I_{PF}, I_{RMP}, I_P represent the PF coil current, the RMP coil current and the plasma current, respectively). As the plasma current influence is mixed with the true value, we adopt an empirical value as the correction factor γ. The γ in the W_{dia} measurement may not be precise and might cause the 2 KJ deviation. The deviation may have a little influence on the calculation, but it will not change the tendency of the δE with power or electron density. The 10 KJ fluctuation amplitude of δE seems a little bit large, as the plasma current distributes in the center for the ohmic discharge case. As the external magnetic probe may not be sensitive to the center information, the W_{mhd} given by EFIT may have larger accidental errors with external magnetic probe for the ohmic case. With LHW power increase, the current distribution will expand to the edge and the accidental errors will decrease.

Figure 4 shows the statistical properties of the heating power dependence of the anisotropic effects on energy. As the factor σ has a larger dispersion in the 0 MW power case due to the large experimental errors, the figure does not show σ

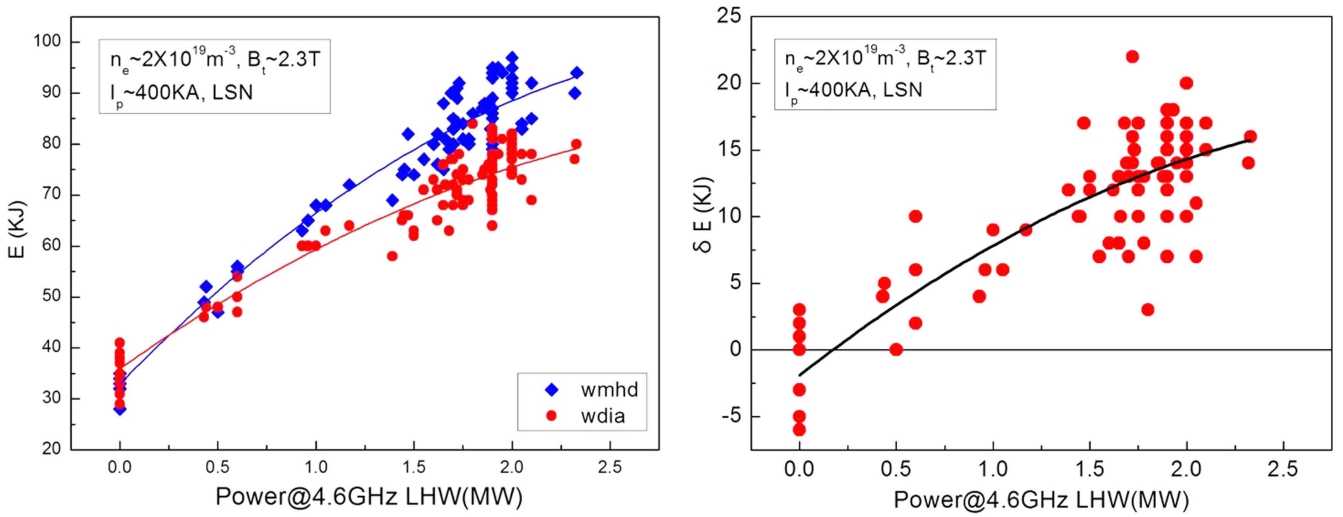

Figure 3. Heating power dependence of W_{mhd}, W_{dia} and δE. Here $\delta \mathrm{E} = W_{\mathrm{mhd}} - W_{\mathrm{dia}}$. In these shots, the toroidal magnetic field is about 2.3 T, the plasma current is about 400 KA, the electron density is about 2×10^{19} m^{-3} and the configuration is LSN.

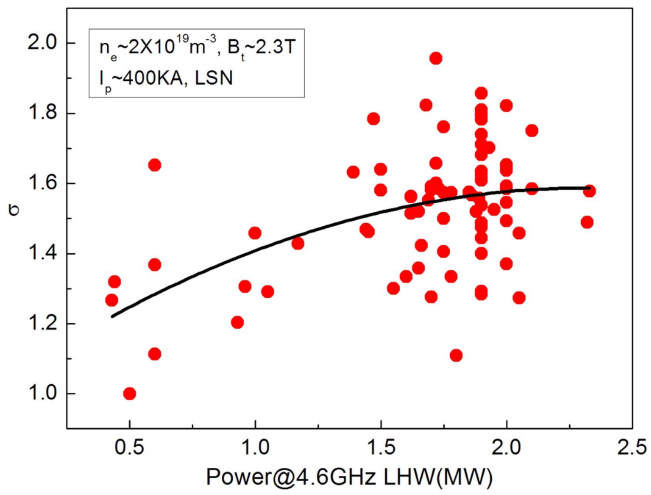

Figure 4. The LHW heating power dependence of the anisotropic effects on energy. The anisotropic factor σ is the ratio of double parallel and perpendicular components of the plasma energy. In these shots, the toroidal magnetic field is about 2.3 T, the plasma current is about 400 KA, the electron density is about 2×10^{19} m^{-3} and the configuration is LSN.

for ohmic discharges. The degree of anisotropy has a positive correlation with heating power, while the increase rate of anisotropic degree slows down at high power.

3.3. Electron temperature influence on the anisotropic effects on energy

To study the electron temperature influence, electron cyclotron resonance frequency heating (ECRH) is used for the 4.6 GHz LHW plasmas. We selected three L mode discharges with almost the same parameters (table 1). Figure 5 shows the variation of W_{mhd} and W_{dia} for each shot. Here:

$$\Delta E\_1 = W'_{\mathrm{mhd}} - W_{\mathrm{mhd}} \tag{7}$$

$$\Delta E\_2 = W'_{\mathrm{dia}} - W_{\mathrm{dia}} \tag{8}$$

$$\Delta \mathrm{E}\_12 = \Delta \mathrm{E}\_1 - \Delta \mathrm{E}\_2. \tag{9}$$

W_{mhd} and W_{dia} are the average value of 0.5 s when 0.1 s before the ECRH switched on. W'_{mhd} and W'_{dia} are the average value of 0.5 s when 0.3 s after the ECRH switched on.

With additional ECRH, W_{mhd} and W_{dia} deduced from the EFIT code and diamagnetic measurement increased by almost a dozen KJ, and the increments of W_{mhd} are slightly larger than the increments of W_{dia}, which means the increments of plasma parallel energy are larger than the perpendicular components.

In comparison to only 4.6 GHz LHW plasmas, the discrepancy between W_{mhd} and W_{dia} and the factor σ with or without ECRH heating are calculated for each shot as shown in figure 6. With ECRH effects, the δE′ is larger than the δE for each shot, while the relative factor σ remains almost unchanged. That is, the degree of the anisotropic effects remains almost unchanged with ECRH in the case of these three shots. The ECRH heats the electrons resulting in higher perpendicular velocities to make the increments of $W_{\perp}$ larger than the increments of $2^{*}W_{\parallel}$ [20]. At the same time, the background electron temperature increases and more electrons will distribute in the acceleration phase velocity of the wave [14]. As a result, more electrons can absorb the LHW energy to make the increments of $2^{*}W_{\parallel}$ larger than the increments of $W_{\perp}$. When the effects of the latter mechanism is slightly larger than the previous one, the degree of the anisotropic effects remains almost unchanged with ECRH. If we can eliminate the perpendicular velocity influence of ECRH, it would be an expected result that only with the electron temperature increasing, the degree of the anisotropic effects on energy induced by 4.6 GHz LHW heating increases.

Table 1. The discharge parameters of EAST shot #56326; #56008; #56005.

Shot number	I_p (KA)	B_t (T)	N_e (10^{19} m^{-3})	Divertor configuration	Power@4.6 GHz LHWs (MW) (&time)	Power@ECRH (MW) (&time)
56326	508	2.5	1.8	LSN	2.4 (1 s ~ 8.5 s)	0.5 (5.5 s ~ 7.5 s)
56008	508	2.5	1.8	LSN	2.5 (2.5 s ~ 8.5 s)	0.5 (5 s ~ 6.5 s)
56005	508	2.5	1.9	LSN	2.4 (2.5 s ~ 8.5 s)	0.5 (4 s ~ 5.5 s)

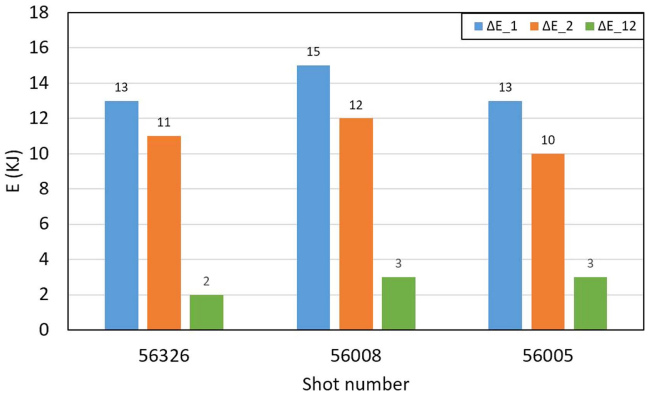

Figure 5. Variation of W_{mhd} and W_{dia} with ECRH heating effects. The ΔE_1 represents the discrepancy between W'_{mhd} (ECRH switched on) and W_{mhd} (ECRH switched off); the ΔE_2 represents the discrepancy between W'_{dia} (ECRH switched on) and W_{dia} (ECRH switched off); the ΔE_12 represents the discrepancy between ΔE_1 and ΔE_2.

4. Conclusion and discussion

By comparing two kinds of calculation energy, the anisotropic effects on energy induced by 4.6 GHz LHW heating on EAST has been studied for the first time in the present work. The statistical properties show an obvious inverse correlation between anisotropic degree and electron density. And the anisotropic degree is in positive correlation with LHW heating power in the L mode. Particularly the degree of the anisotropic effect can reach $2^*W_{\|}/W_{\perp} \sim 1.8$ at low electron density with LHW heating. This quantitative evaluation of the plasma anisotropy may be helpful in the EAST future equilibrium and instabilities analysis.

In the diamagnetic flux measurement, the correction factor γ may not be precise. And the experimental errors may be a little bit large at the ohmic discharge, as the plasma current distributes in the center. But with the LHW heating power increases, the experimental errors will reduce, while the plasma energy increases. The impacts of the measurement errors become smaller at higher heating power.

The density impact on anisotropy may have two major mechanisms: one is the collision frequency influence. In the higher density operation, the electron temperature is lower and the collision frequency is higher. The high-energy electron slowing down time is shorter. And more energy will be transferred to perpendicular direction by collision. Hence $W_{\perp}$ (or W_{dia}) increase with density increase as figure 1 shows. Another mechanism may be the LHW power coupling. Due to a complex problem of coupling between fast waves and plasma particles (collisions, parametric instabilities, accessibility, etc) [13], significant LHW power can be lost at the plasma edge, especially in a high-density plasma [21]. That is, the LHW heating efficiency will decrease with increasing density. As a result, the absorbed LHW energy will reduce and the plasma total energy (W_{mhd}) will decrease with increasing density (figure 1). This mechanism is similar to the LHW power dependence case.

The positive correlation between anisotropic degree and the LHW heating power is expected because the anisotropy is induced by LHW heating. With power increase, the parallel energy increase rate will be larger than the perpendicular energy increase rate, then the anisotropic degree increases. In addition, the anisotropic degree increase rate will reduce at high LHW heating power, especially when the heating power exceeds 2 MW (see figure 4, the σ increase tendency). One possible reason may be due to the plasma confinement performance. Due to the L mode having a degradation of confinement with increasing auxiliary heating power [22], the high-energetic electrons generated by LHW heating will lose faster at high power. Although the increasing power can generate more high-energetic electrons, a larger proportion of high-energetic electrons will be lost before slowing down as the energy confinement time decreases. This process ultimately results in the anisotropic degree increase slowing down at high LHW heating power.

The current drive by the combined effects of lower-hybrid and electron-cyclotron absorption has been studied in recent research [23–25]. By analyzing combination experiments of LHW and ECRH, the ECRH heating effects on energy in 4.6 GHz LHW plasma are also studied on EAST. The synergy between LH and electron cyclotron can be shown from the anisotropic degree change. In general, the acceleration phase velocity of the LHW is selected in the high electron velocity region. In the experimental case, there are two mechanisms: the ECHR triggers higher perpendicular velocities and the LHW Landau damping effects trigger higher parallel velocities with more high-energy electrons generated by the ECRH. When the previous mechanism dominates, the degree of the anisotropic effects will decrease with ECRH heating switched on. While the latter one dominates, the anisotropic degree will increase. And in the experimental case, the anisotropic degree remains almost unchanged. In other words, the high background electron temperature could be favorable to high LHW heating efficiency.

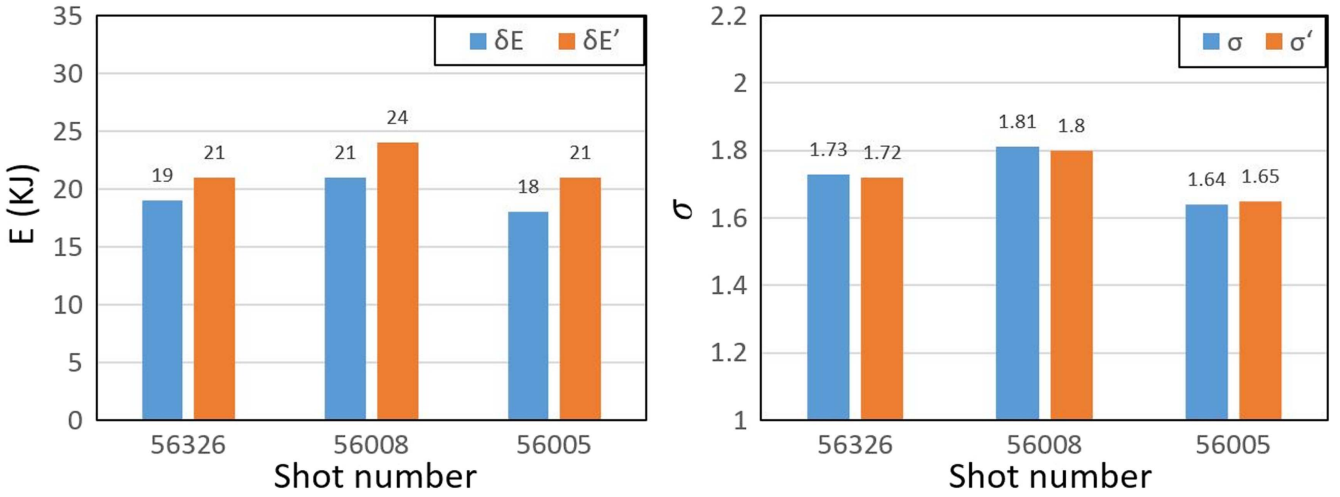

Figure 6. ECRH heating effects on energy in 4.6 GHz LHWs plasma. The δE and δE′ denote the discrepancy between W_{mhd} and W_{dia} (ECRH switched off) and the discrepancy between W'_{mhd} and W'_{dia} (ECRH switched on), respectively. The σ and σ' denote $2^{*}W_{||}/W_{\perp}$ (ECRH switched off) and $2^{*}W_{||}{}'/W_{\perp}{}'$ (ECRH switched on), respectively.

Acknowledgments

This work is supported by the National Magnetic Confinement Fusion Science Program of China under Grant No. 2013GB106003B and No.2015GB102004.

References

[1] Goldston R J 1984 Energy confinement scaling in tokamaks: some implications of recent experiments with ohmic and strong auxiliary heating *Plasma Phys. Control. Fusion* **26** 87
[2] Catto P J and Simakov A N 2004 A drift ordered short mean free path description for magnetized plasma allowing strong spatial anisotropy *Phys. Plasmas* **11** 90–102
[3] Fitzgerald M *et al* 2015 MHD normal mode analysis with equilibrium pressure anisotropy *Plasma Phys. Control. Fusion* **57** 025018
[4] Qu Z S *et al* 2014 Analysing the impact of anisotropy pressure on tokamak equilibria *Plasma Phys. Control. Fusion* **56** 075007
[5] Cooper W A *et al* 2006 Anisotropic pressure bi-Maxwellian distribution function model for three-dimensional equilibria *Nucl. Fusion* **46** 683–98
[6] Graves J P *et al* 2003 The internal kink mode in an anisotropic flowing plasma with application to modeling neutral beam injected sawtoothing discharges *Phys. Plasmas* **10** 1034–47
[7] Berkery J W *et al* 2014 The effect of an anisotropic pressure of thermal particles on resistive wall mode stability *Phys. Plasmas* **21** 112505
[8] Gorelenkov N N *et al* 2005 Beam anisotropy effect on Alfvén eigenmode stability in ITER-like plasmas *Nucl. Fusion* **45** 226–37
[9] Zwingmann W *et al* 2001 Equilibrium analysis of tokamak discharges with anisotropic pressure *Plasma Phys. Control. Fusion* **43** 1441–56
[10] Hole M J *et al* 2011 Identifying the impact of rotation, anisotropy, and energetic particle physics in tokamaks *Plasma Phys. Control. Fusion* **53** 074021
[11] Qi L *et al* 2013 Simulation of linear and nonlinear Landau damping of lower hybrid waves *Phys. Plasmas* **20** 062107
[12] Fisch N J 1987 Theory of current drive in plasmas *Rev. Mod. Phys.* **59** 175–234
[13] Bonoli P T 2014 Review of recent experimental and modeling progress in the lower hybrid range of frequencies at ITER relevant parameters *Phys. Plasmas* **21** 061508
[14] ITER physics Expert Groups 1999 Chapter 6: plasma auxiliary heating and current drive *Nucl. Fusion* **39** 2495–539
[15] Wu S 2007 An overview of the EAST project *Fusion Eng. Des.* **82** 463–71
[16] Liu F K *et al* 2015 First results of LHCD experiments with 4.6 GHz system toward steady-state plasma in EAST *Nucl. Fusion* **55** 123022
[17] Qian J P *et al* 2009 Equilibrium reconstruction in EAST tokamak *Plasma Sci. Technol.* **11** 142
[18] Lao L L *et al* 1990 Equilibrium analysis of current profiles in tokamaks *Nucl. Fusion* **30** 1035–49
[19] Lao L L *et al* 1985 Separation of $\overline{\beta_p}$ and l_i in tokamaks of non-circular cross-section *Nucl. Fusion* **25** 1421–36
[20] Erckmann V and Gasparino U 1994 Electron cyclotron resonance heating and current drive in toroidal fusion plasmas *Plasma Phys. Control. Fusion* **36** 1869–962
[21] McWilliams R *et al* 1980 Steady-state currents driven by collisionally damped lower-hybrid waves *Phys. Rev. Lett.* **44** 245–8
[22] ITER physics Expert Groups 1999 Chapter 2: plasma confinement and transport *Nucl. Fusion* **39** 2175–249
[23] Fidone I *et al* 1984 Current drive by the combined effects of electron-cyclotron and Landau wave damping in tokamak plasmas *Phys. Fluids* **27** 2468
[24] Dumont R J and Giruzzi G 2004 Theory of synergy between electron cyclotron and lower hybrid waves *Phys. Plasmas* **11** 3449–59
[25] Giruzzi G *et al* 2004 Synergy of electron-cyclotron and lower-hybrid current drive in steady-state plasmas *Phys. Rev. Lett.* **93** 255002